

# Enhancing the oxygen vacancy formation and migration in bulk chromium (III) oxide by alkali metal doping: A change from isotropic to anisotropic oxygen diffusion

John J. Carey <sup>a</sup> and Michael Nolan <sup>a</sup>

<sup>a</sup> Tyndall National Institute, University College Cork, Lee Maltings Complex, Dyke Parade, Cork, Ireland, T12 R5CP

## Supporting Information

### Compensated oxygen vacancy formation energies for doped Cr<sub>2</sub>O<sub>3</sub>

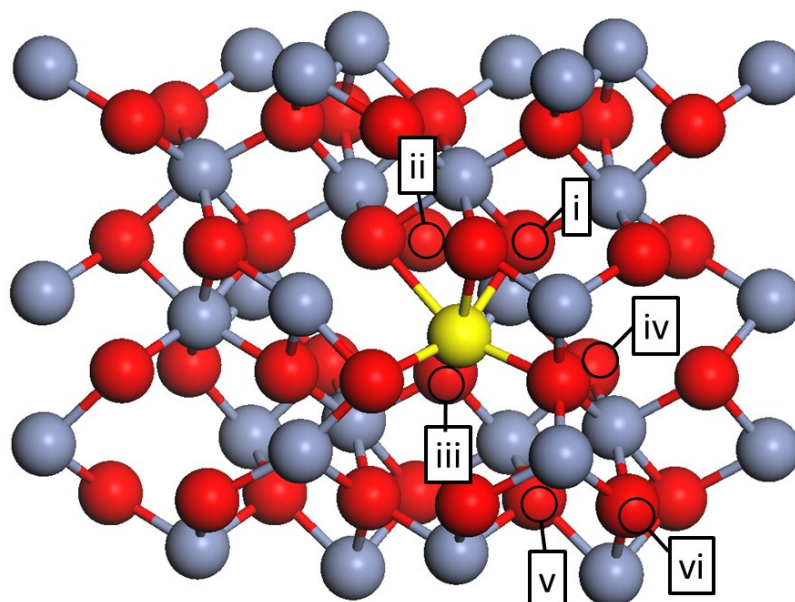
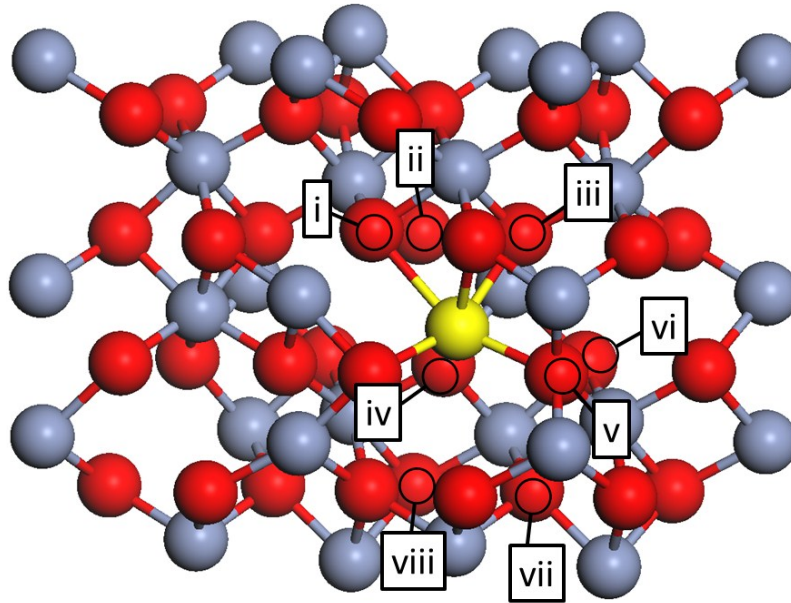


Figure 1: The lattice oxygen atoms examined for oxygen vacancy compensation in Li-Cr<sub>2</sub>O<sub>3</sub>. Symmetrically equivalent atoms are not considered. Yellow sphere is the relative position of the dopant cation.

Table 1: The calculated energies for the different oxygen atoms examined for compensation in Figure 1 for Li-Cr<sub>2</sub>O<sub>3</sub>

	$E[\text{comp}] + 1/2 E[\text{O}_2] - E[\text{M-Cr}_2\text{O}_3]$ (eV)
<b>i</b>	0.77
<b>ii</b>	1.72
<b>iii</b>	0.71
<b>iv</b>	1.84
<b>v</b>	2.12
<b>vi</b>	3.21



**Figure 2:** The lattice oxygen atoms examined for oxygen vacancy compensation in Na-Cr<sub>2</sub>O<sub>3</sub>. Symmetrically equivalent atoms are not considered. Yellow sphere is the relative position of the dopant cation

**Table 2:** The calculated energies for the different oxygen atoms examined for compensation in Figure 2 for Na-Cr<sub>2</sub>O<sub>3</sub>

	$E[\text{comp}] + 1/2 E[\text{O}_2] - E[\text{M-Cr}_2\text{O}_3]$ (eV)
<b>i</b>	1.98
<b>ii</b>	2.41
<b>iii</b>	2.08
<b>iv</b>	1.34
<b>v</b>	0.69
<b>vi</b>	1.16
<b>vii</b>	2.49
<b>viii</b>	2.49

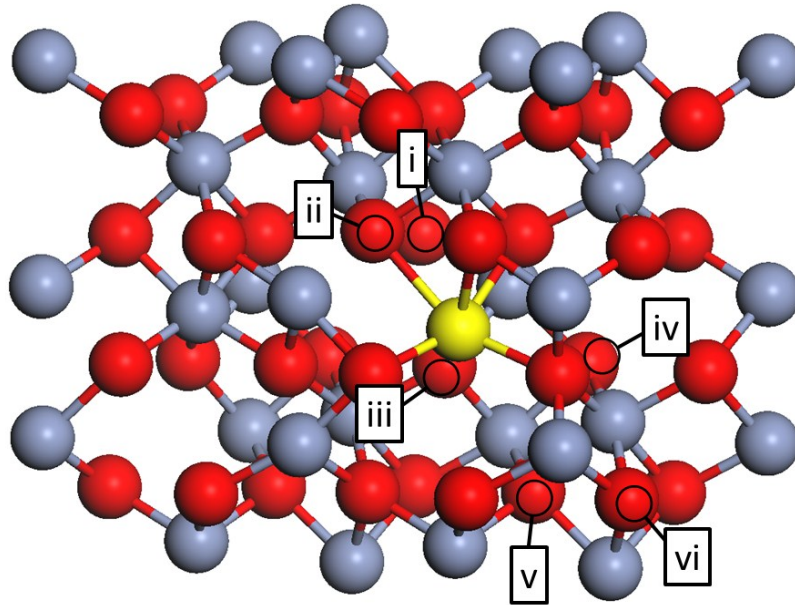
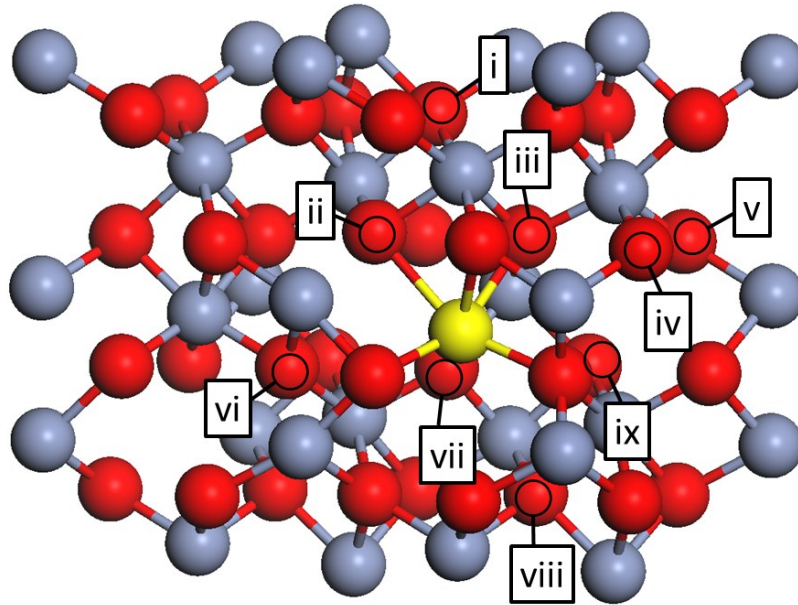


Figure 3: The lattice oxygen atoms examined for oxygen vacancy compensation in  $\text{K-Cr}_2\text{O}_3$ . Symmetrically equivalent atoms are not considered. Yellow sphere is the relative position of the dopant cation.

Table 3: The calculated energies for the different oxygen atoms examined for compensation in Figure 3 for  $\text{K-Cr}_2\text{O}_3$

	$E[\text{comp}] + 1/2 E[\text{O}_2] - E[\text{M-Cr}_2\text{O}_3]$ (eV)
<b>i</b>	1.97
<b>ii</b>	1.03
<b>iii</b>	-0.04
<b>iv</b>	2.18
<b>v</b>	2.89
<b>vi</b>	2.89



**Figure 4:** The lattice oxygen atoms examined for oxygen vacancy compensation in Rb-Cr<sub>2</sub>O<sub>3</sub>. Symmetrically equivalent atoms are not considered. Yellow sphere is the relative position of the dopant cation.

**Table 4:** The calculated energies for the different oxygen atoms examined for compensation in Figure 4 for Rb-Cr<sub>2</sub>O<sub>3</sub>

	$E[\text{comp}] + 1/2 E[\text{O}_2] - E[\text{M-Cr}_2\text{O}_3]$ (eV)
<b>i</b>	2.44
<b>ii</b>	1.78
<b>iii</b>	1.98
<b>iv</b>	2.56
<b>v</b>	2.80
<b>vi</b>	2.80
<b>vii</b>	0.13
<b>viii</b>	3.01
<b>ix</b>	2.69

## Active oxygen vacancy formation energies for doped Cr<sub>2</sub>O<sub>3</sub>

The distribution of oxygen vacancies for the ‘active’ oxygen species in each doped system is explored in a similar way to Figures 1 – 4 above; in the oxygen layers above, same layer and layer below the dopant in the compensated structure. Note the lattice oxygen explored for active vacancy formation are not the exact same oxygens as shown above since the geometry and symmetry has changed from the uncompensated structures to the compensated structures due to local distortions induced by the removal of the first lattice oxygen atom. The approach in exploring numerous positions is similar. Only the energies are given below.

**Table 5: The calculated energies for the distribution of active oxygen vacancies in each of the doped structures**

		<b>Li-Cr<sub>2</sub>O<sub>3</sub></b> <b>E[active]</b> <b>(eV)</b>	<b>Na-Cr<sub>2</sub>O<sub>3</sub></b> <b>E[active]</b> <b>(eV)</b>	<b>K-Cr<sub>2</sub>O<sub>3</sub></b> <b>E[active]</b> <b>(eV)</b>	<b>Rb-Cr<sub>2</sub>O<sub>3</sub></b> <b>E[active]</b> <b>(eV)</b>
<b>Layer above dopant</b>	<b>i</b>	4.61	2.27	2.56	2.61
	<b>ii</b>	3.81	2.44	2.62	1.74
	<b>iii</b>	2.71	2.39	3.11	2.63
<b>Same layer as dopant</b>	<b>iv</b>	4.60	3.09	4.65	1.63
	<b>v</b>	4.44	2.78	3.38	2.60
	<b>vi</b>	4.44	3.58	3.39	2.60
	<b>vii</b>	3.28	---	2.14	2.43
	<b>viii</b>	3.28	---	---	2.61
<b>Layer below dopant</b>	<b>ix</b>	4.64	3.30	3.58	1.09
	<b>x</b>	5.50	3.33	3.53	2.71
	<b>xi</b>	---	---	---	2.91
	<b>xii</b>	---	---	---	2.57

## Oxygen migration graphs for doped $\text{Cr}_2\text{O}_3$

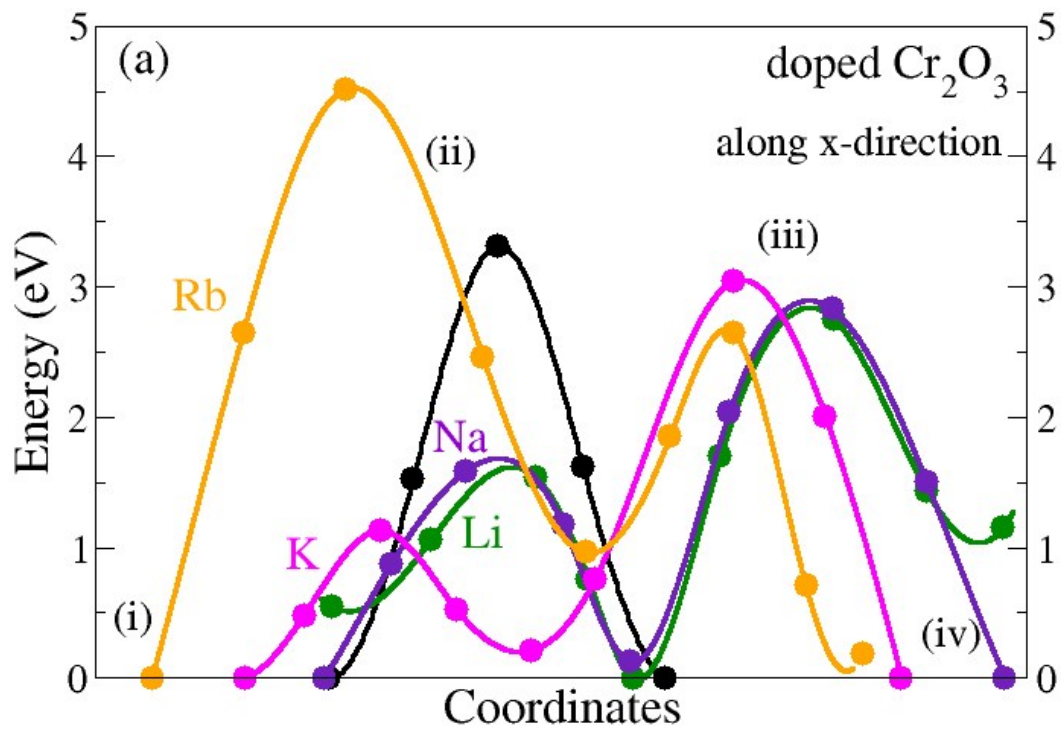


Figure 5: The calculated oxygen migration pathways along the [010] direction. The graph is plotted by the change in energy with respect to the change in the x coordinate along the [010] direction.

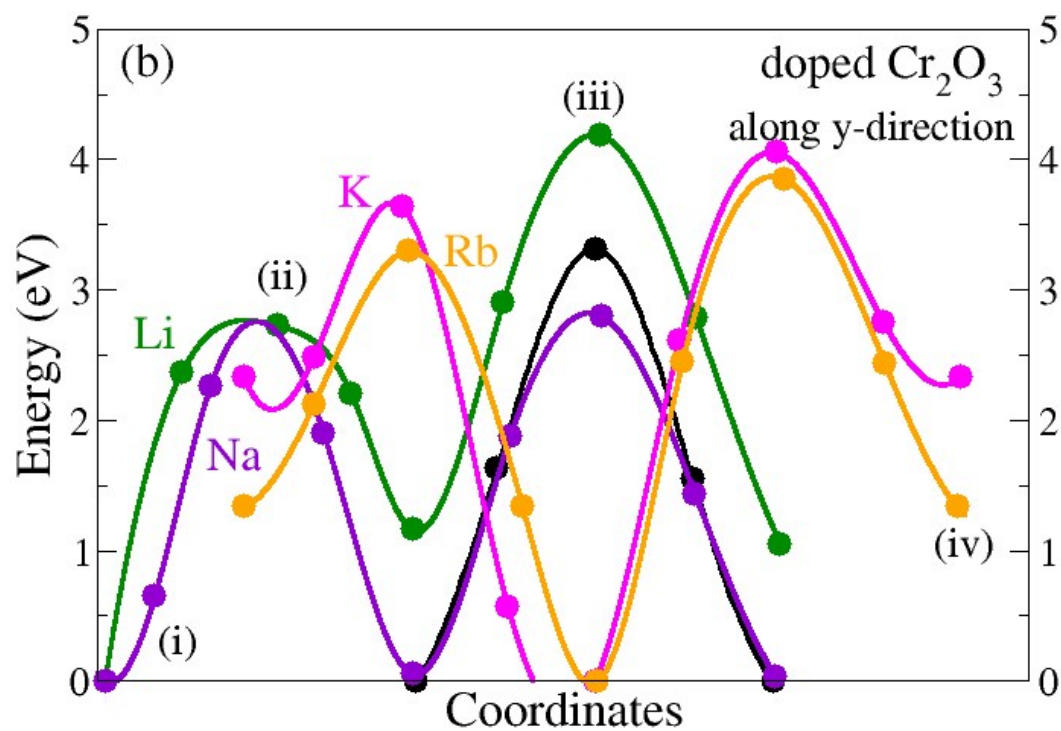


Figure 6: The calculated oxygen migration pathways along the [100] direction. The graph is plotted by the change in energy with respect to the change in the y coordinate along the [010] direction

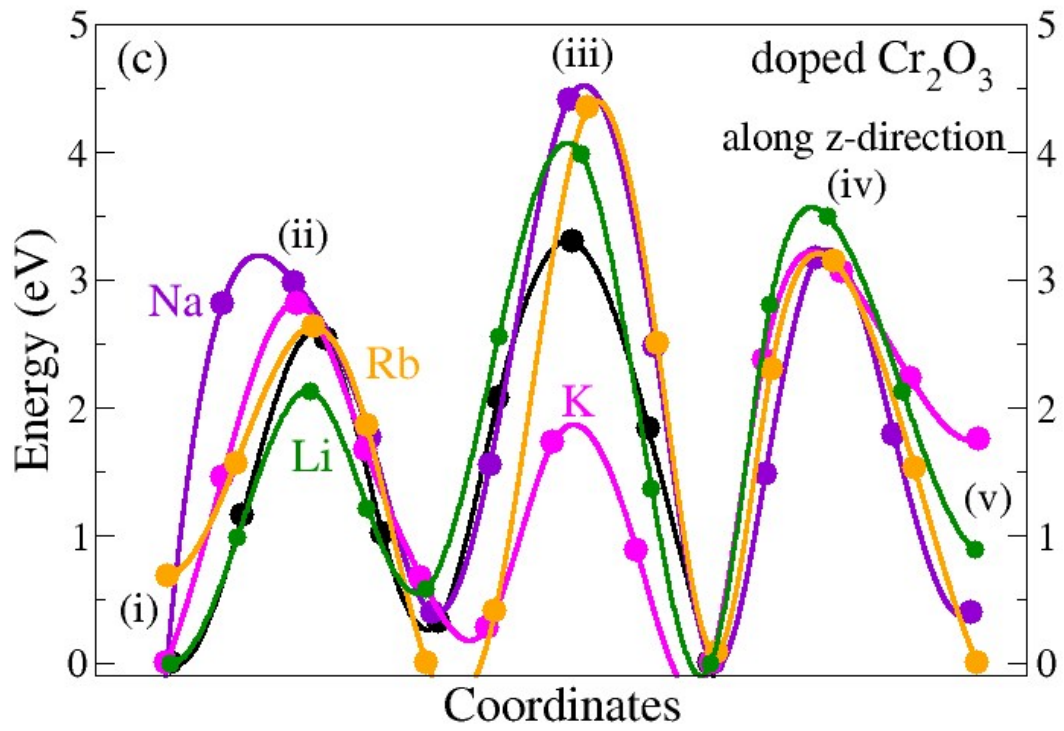


Figure 7: The calculated oxygen migration pathways along the [110] direction. The graph is plotted by the change in energy with respect to the change in the z coordinate along the [110] direction.